Clays and Clay Minerals, Vol. 42, No. 2, 123–136, 1994.

THE EFFECT OF SURFACE MODIFICATION BY AN ORGANOSILANE ON THE ELECTROCHEMICAL PROPERTIES OF KAOLINITE

BELINDA BRAGGS, DANIEL FORNASIERO, JOHN RALSTON, AND ROGER ST. SMART

School of Chemical Technology, University of South Australia
The Levels, S.A. 5095, Australia

Abstract—The electrochemical properties of kaolinite before and after modification with chlorodimethyloctadecylsilane have been studied by electrophoretic mobility, surface charge titration, and extrapolated yield stress measurements as a function of pH and ionic strength. A heteropolar model of kaolinite, which views the particles as having a pH-independent permanent negative charge on the basal planes and a pH-dependent charge on the edges, has been used to model the data. The zeta potential and surface charge titration experimental data have been used simultaneously to calculate acid and ion complexation equilibrium constants using a surface complex model of the oxide-solution interface. The experimental data were modeled following subtraction of the basal plane constant negative charge, describing only the edge electrical double layer properties. Extrapolated yield stress measurements along with the electrochemical data were used to determine the edge isoelectric points for both the unmodified and modified kaolinite and were found to occur at pH values of 5.25 and 6.75, respectively. Acidity and ion complexation constants were calculated for both sets of data before and after surface modification. The acidity constants, $pKa_1 = 5.0$ and $pKa_2 = 6.0$, calculated for unmodified kaolinite, correlate closely with acidity constants determined by oxide studies for acidic sites on alumina and silica, respectively, and were, therefore, assigned to pH-dependent specific chemical surface hydroxyl groups on the edges of kaolinite. The parameters calculated for the modified kaolinite indicate that the silane has reacted with these pH-dependent hydroxyl groups causing both a change in their acidity and a concomitant decrease in their ionization capacity. Infrared data show that the long chain hydrocarbon silane is held by strong bonding to the kaolinite surface as it remains attached after washing with cyclohexane, heating, and dispersion in an aqueous environment.

Key Words—Acidity constants, Electrophoresis, Kaolinite, Modeling, Silane, Surface charge, Surface modification.

INTRODUCTION

Kaolinite is a mineral that has a wide variety of applications in industry, particularly as a paper filler and a coating pigment (Jepson, 1984). It is used as an extender in water based paints and ink, as a functional additive in polymers and is a major component of ceramics (Jepson, 1984). Kaolinite is an inexpensive additive that can improve the properties of the material in which it is dispersed provided that a stable dispersion is formed. In order to achieve this state, the kaolinite surface is usually modified in some way. The surface interactions that occur at the interface when this mineral is incorporated into aqueous dispersions or polymer systems are poorly understood. For example, the development of surface charge in aqueous systems and, consequently, the electrical double layer properties of the surface as a function of pH and ionic strength have not been critically examined before and after surface modification. Therefore, the aim of this study is to examine the electrochemical and rheological properties of a well-ordered, pure kaolinite before and after surface modification with an organosilane. Complementary infrared spectroscopic studies are included to provide evidence as to the mode of attachment of the organosilane. The electrochemical properties of both the unmodified and modified kaolinite have been investigated by both electrophoretic mobility measurements and surface charge titrations and the rheological properties have been investigated by extrapolated yield stress measurements, thereby providing a comprehensive picture of the electrical double layer properties. In order to interpret the data, one needs to be aware that kaolinite is a mixed oxide system, rather than a single pure oxide favored in the vast majority of electrical double layer investigations (Hunter, 1987; James and Parks, 1982).

Kaolinite is a 1:1 dioctahedral aluminosilicate that has two different basal cleavage faces (Hurlbut, 1971). One basal face consists of a tetrahedral siloxane surface with very inert –Si–O–Si– links. The other basal surface consists of an octahedral, gibbsite ($Al(OH)_3$) sheet. Both of these surfaces are theoretically electrically neutral. At the edges of a 1:1 layer, the structure is disrupted and broken bonds occur that are accommodated as OH groups. These edges are estimated to occupy approximately 10% of the whole kaolinite surface (Williams and Williams, 1978; Wierer and Dobias, 1988). The kaolinite surface has a complex chemistry due to the

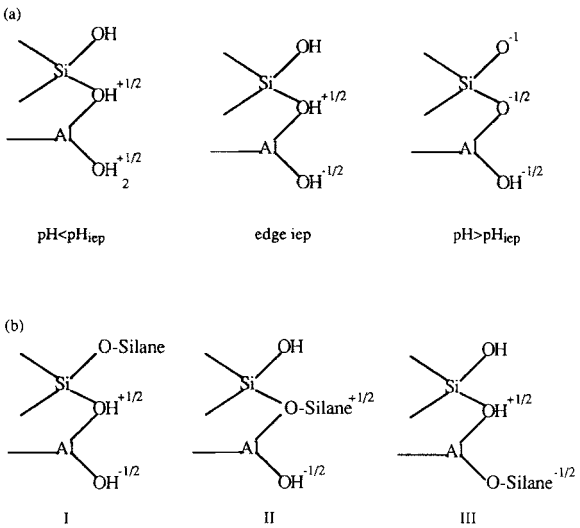

Figure 1. a) The charge on the broken edges of a kaolinite particle as a function of the pH. b) Three possible products (I, II, III) after reaction of an organosilane with the hydroxyl groups at the broken edges of kaolinite particles.

existence of these different sites on the basal faces and edges. It has been shown to adsorb H^+ and OH^- as potential determining ions (pdi) in aqueous solution. Wierer and Dobias (1988) provide calorimetric evidence that it is the edge sites that are responsible for the adsorption of these potential determining H^+ and OH^- ions in aqueous solutions with the basal faces showing no detectable interaction with H^+ or OH^-. Kaolinite also shows cation adsorption that increases with increasing pH and a small anion adsorption that decreases with increasing pH (Jepson, 1984). The anion and some of the cation adsorption are attributed to the edge sites that are considered to be positively charged at low pH, neutral at the edge isoelectric point (edge iep), and negatively charged at higher pH as shown in Figure 1a (Jepson, 1984; Greenland and Mott, 1978). The remainder of the cation adsorption is attributed to the basal planes, and Jepson (1984) summarizes the three extant theories that purportedly account for the origin of the remainder of the cation adsorption and the view that the basal planes carry a permanent negative charge. The first suggests that the siloxane surface carries a permanent negative charge due to isomorphous replacement of Al for Si. The second proposes that the kaolinite contains small amounts of adsorbed, expanding 2:1 layer minerals such as vermiculite and smectite causing the basal surfaces to have a constant negative charge. The third view is that aluminosilicate gel coatings, rich in silica, may exist on the surface, conferring a negative charge on the basal surface that becomes more negative with increasing pH. It is the variation of these different charge contributions at the basal surfaces and at the edges with pH and ionic strength that is used to account theoretically for the measured changes in electrophoretic mobility, surface charge, and extrapolated yield strength as a function of pH and ionic strength (Diz and Rand, 1989; Bolland *et al.*, 1980; Rand and Melton, 1977; van Olphen, 1977; Schofield and Samson, 1954).

The hydroxyl groups at the plate edges are considered to be the major reactive sites (Morris *et al.*, 1990). At the edges, there are three possible hydroxyl sites available for reaction with chlorosilanes (Figure 1b), the Si–OH (I), the Si–$OH^{+½}$–Al (II) and the Al–$OH^{-½}$ (III). There has been no published evidence for the mechanism or actual locations at which organosilanes or other species react with kaolinite. Previous work has generally focused on silica, and the common view is that chlorosilanes react with the surface silanol groups, Si–OH, to form –Si–O–SiR_3 links (Pleuddemann, 1982; Hair, 1986). Morris *et al.* (1990) have provided Al^{27} NMR spectroscopic evidence that the octahedral edge Al–OH Brönsted acid sites of Fe-bearing montmorillonite clays react with trimethylchlorosilane. Hence, in kaolinite it may be that one or more of the hydroxyl sites are involved in chemical reactions at the edges. By reacting kaolinite with a monochlorosilane, examining the surface by FTIR, studying the rheological characteristics, and comparing the zeta potential and surface charge characteristics of the modified and unmodified surfaces in this paper, a mechanism is proposed by which monochlorosilanes react with the surface of kaolinite and the subsequent effect of this modification on the electrical double layer properties is discussed.

EXPERIMENTAL PROCEDURES

Materials

The kaolinite, Hydrite PX, used in this study was supplied by the Georgia Kaolin Company. Hydrite PX is a well ordered, water processed kaolinite of greater than 97% purity. In the process used by the Georgia Kaolin Company to purify the kaolinite, the particles were cleaved to expose fresh surfaces, then water washed to remove any soluble impurities. Ninety percent by weight of the kaolinite particles have an equivalent spherical diameter (e.s.d.) of less than 2 μm, with a median particle size of 0.7 μm and a specific surface area of 15.3 ± 0.5 $m^2\ g^{-1}$ (B.E.T. N_2 Adsorption). The pH of a 0.1% aqueous slurry is 5. The cation exchange capacity (CEC) is 3.1 meq 100 g^{-1}. Examination by X-ray photoelectron spectroscopy did not detect any surface contamination. The kaolinite was, therefore, used without further treatment. The silane used to modify the surface of the kaolinite was AR grade chlorodimethyloctadecylsilane. This was used without further purification. AR grade reagents (HNO_3, KOH, KNO_3) were used for all surface charge, electrophoretic mobility, and rheological measurements. High purity,

https://doi.org/10.1346/CCMN.1994.0420203 Published online by Cambridge University Press

oxygen-free nitrogen (CIG > 99.99%) was bubbled successively through a solution of 0.1 mol dm^{-3} KOH, a precipitated silica (BDH) suspension, conductivity (high purity, $\kappa \leq 0.5 \times 10^{-6}\ \Omega^{-1}\ cm^{-1}$, $\gamma = 72.8\ mNm^{-1}$ at 20°C) water prior to entering the temperature controlled (25°C) vessels used in the electrical double layer measurements. All glassware was soaked in 2 mol dm^{-3} KOH, rinsed repeatedly with distilled water and conductivity water, and then steamed and dried before use. All solutions were made with conductivity water freshly prepared by reverse osmosis followed by passage through a mixed bed ion exchange resin and then activated charcoal prior to a final 0.22 μm filter.

Preparation of surface modified kaolinite

The kaolinite was dried in a clean oven at 110°C for 2.5 h prior to reaction with the silane. Six g of kaolinite was stirred in 50 cm^3 of a 50% v/v silane and cyclohexane solution for 2 hr in a quick-fit conical flask with a drying tube containing anhydrous calcium chloride in the neck of the flask. After reaction, the sample was filtered and dried under vacuum then washed with cyclohexane, filtered, and dried under vacuum twice to remove any residual unreacted silane. The sample was subsequently dried in an oven at 110°C overnight and then stored in a desiccator over silica gel. This sample is referred to as "C18-kaolin," indicating that the silane used has a long carbon chain of 18 attached to the silica atom as well as two methyl groups. The unmodified kaolinite is referred to as "u-kaolin."

Infrared spectroscopy

Diffuse reflectance spectra were recorded using a BIORAD model FTS-65 spectrometer equipped with a Spectra Tech diffuse reflectance accessory and an MCT detector. All spectra were recorded at room temperature in absorbance mode at 4 cm^{-1} resolution, and 256 scans were taken. Dried and ground spectroscopic grade KBr was used as a background. Samples were mixed with the same KBr to make a 3% by weight dilution in order to prevent the large inversion of bands due to specular reflectance (Messerschmidt, 1985; Nguyen *et al.*, 1991), which occurs in the region below 1500 cm^{-1} in kaolinite samples.

Spectra were recorded for u-kaolin and C18-kaolin after drying at 110°C for 18 hr. A sample of the C18-kaolin, left in the conditioning vessel after completion of electrophoresis measurements, was removed from the vessel, centrifuged, and dried. This sample was examined by infrared to show that the silane was still present on the kaolinite after being stirred in the aqueous environments used for electrophoresis and surface charge measurements.

Electrophoretic mobility measurements

Electrophoretic mobilities were measured using a Malvern Zetasizer Model 2c instrument. Five hundred cm^3 of 0.1% suspensions of kaolinite were conditioned for 1.5 hr at 25°C. Trials performed on the u-kaolin showed that the results were reproducible for conditioning times of 1.5 to 24 hr. The suspensions were stirred continuously, and N_2 was bubbled through the suspensions during both conditioning and the measurement. The electrolyte used was KNO_3 at ionic strengths of either 0.01 mol dm^{-3} or 0.001 mol dm^{-3}. The pH of the suspension was adjusted using dilute HNO_3 and KOH. The pH ranged from approximately 2.7 to 10 for 0.01 mol dm^{-3} KNO_3 solutions and approximately 3.6 to 10 for 0.001 mol dm^{-3} KNO_3 solutions. Ten cm^3 samples were removed with a syringe at approximately 0.5 pH intervals. Three separate 2 cm^3 samples were immediately injected into the electrophoresis cell, electrophoretic mobility measurements were recorded, and an average value taken. Electrophoretic mobility was converted to zeta potential using the Ohshima *et al.* (1983) approach; however, there was no significant difference in the calculated zeta potentials when the Smoluckowski equation (Hunter, 1981, 1987) was used. The average error in the measurement of the three samples at each pH was ±2 mV.

Surface charge titrations

Surface charge titrations were performed on samples of u-kaolin and C18-kaolin using a Metrohm Model 670 titroprocessor coupled to a Model 665 Dosimat delivering prescribed quantities of either acid or base. A Metrohm A6 100 Herisau combined glass electrode was connected to the titroprocessor. The concentration of the solid samples used was 20.02 g dm^{-3}. The sample was placed in the reaction vessel, and the 0.001 mol dm^{-3} KNO_3 electrolyte solution was slowly added. The suspensions were conditioned for 1.5 hr at 25°C under N_2 at the natural pH of the sample. The suspension was titrated up to pH 10 using KOH, titrated down to pH 3.5 using HNO_3, then titrated back up to around pH 10.5. The electrolyte concentration was increased to 0.01 mol dm^{-3} KNO_3, and the shift in pH was recorded. This shift was used to position the surface charge curves in relation to each other (Wood, 1990). The suspension was left to equilibrate for 30 min. After equilibration, the suspension was titrated down to around pH 2.8 then back up to around pH 11. This procedure was repeated for 0.1 and 1.0 mol dm^{-3} KNO_3. All titrations were performed in a N_2 atmosphere. The concentration of the acid HNO_3, base KOH and the addition of KNO_3 for each sample was such that the total additions during the four titrations did not alter the volume of the sample significantly. This procedure was repeated in the absence of solid so that blank titrations were available at each electrolyte concentration. The relative surface charge, σ_0 (C m^{-2}), for each sample at each electrolyte concentration was calculated by determining the concentration of the potential determining ions, H^+ and OH^-, adsorbed on

https://doi.org/10.1346/CCMN.1994.0420203 Published online by Cambridge University Press

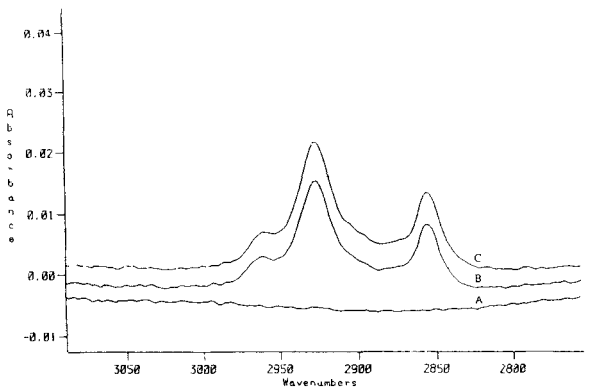

Figure 2. DRIFT spectra of 3% w/w samples in KBr of A) u-kaolin, B) C18-kaolin before and C) after stirring in an aqueous environment. Enlarged view of peaks at 2961 cm^{-1}, 2925 cm^{-1}, and 2855 cm^{-1}.

the surface of that sample according to the equation (de Bruyn and Agar, 1962; Wood, 1990)

$$\sigma_0 = B([H^+] - [OH^-]) \quad (1)$$

where B = F/SC. F is the Faraday constant, S is the surface area in $m^2\ g^{-1}$, and C is the concentration of the sample in g dm^{-3}. The concentrations of H^+ and OH^- adsorbed onto the surface at a particular pH were calculated from the difference between the concentrations of H^+ and OH^- added during the sample and blank titrations. The absolute surface charge was determined by using the shift in pH on addition of electrolyte to position the curves in relation to one another followed by adjustment of all the curves together in order to make the common intersection point (cip) equal to the point of zero charge (Wood, 1990; de Bruyn and Agar, 1962).

Rheological measurements and sedimentation volume determinations

Extrapolated yield stress measurements were determined using a Haake Model CV20 Rheometer fitted with an ME45 Sensor. Ten % w/v suspensions of the solid samples in conductivity water were prepared, taken to a pH of 10, and left for 1.5 hr to equilibrate at 25°C while stirring. Measurements were recorded on samples as the pH was decreased by approximately 0.5 pH units down to approximately pH 2.5. The experiments were repeated at ionic strengths of 0.001 mol dm^{-3}, 0.01 mol dm^{-3}, and 0.1 mol dm^{-3} KNO_3. The rheometer was programmed to increase the shear from 0 to 300 cycles per second (c s^{-1}) in 0.1 min, shear at 300 c s^{-1} for 1 min, return to rest in 0.1 min, and rest for 2 min. This was followed by an increase in shear from 0 to 300 c s^{-1} in 1 min then back to 0 in 1 min, at which time shear stress τ (N m^{-2}) *vs.* shear rate $\dot{\gamma}$(s^{-1}) measurements were recorded.

Sedimentation volumes were determined on samples of unmodified kaolinite to confirm the rheology results. Two hundred cm^3 of 10% w/v suspensions of the kaolinite were prepared in three electrolyte concentrations, no electrolyte, 0.001 mol dm^{-3} KNO_3, and 0.01 mol dm^{-3} KNO_3. The suspensions were taken up to a pH of 10 and stirred for 1.5 hr at 25°C. After this time, the pH was decreased to 7.25 in each of the three suspensions and left for 30 min while stirring. Fifty cm^3 aliquots were removed and placed in measuring cylinders, and paraffin wax paper was used to seal the tops of the measuring cylinders to prevent evaporation. This was repeated at pH values of 5.25 and 3.5. The measuring cylinders were left for two months undisturbed. The percentage volume of sediment was then determined.

RESULTS

Infrared spectroscopy

Figure 2 shows the infrared spectra of (A) the u-kaolin and (B) the C18-kaolin before and (C) after stirring in the aqueous solution. The C18-kaolin shows three bands at 2961 cm^{-1}, 2925 cm^{-1}, and 2855 cm^{-1}, which are not present in the u-kaolin. These three bands can be assigned to the C–H asymmetric stretch of the methyl groups, the C–H asymmetric stretch of the methylene groups and the C–H symmetric stretch of the methylene groups of the silane, respectively (Socrates, 1980). There is no change in the absorbance of the C–H bands in C18-kaolin after stirring in the aqueous environment. These spectra indicate that the organosilane is held by strong bonding to the surface of kaolinite, as neither washing with cyclohexane and drying under vacuum followed by heating at 110°C nor conditioning in an aqueous environment has removed the silane.

Electrophoresis and surface charge titrations

Figure 3 shows the change in zeta potential (ζ) and surface charge (σ_0) of u-kaolin as a function of pH and electrolyte concentration. Both the ζ and σ_0 curves do not vary significantly with electrolyte concentration. Similar behavior for another kaolinite sample has been observed by de Keizer (1990). The isoelectric point (iep) occurs around pH 3. This is in agreement with other studies in which samples of similar purity to this kaolinite sample have been used (de Keizer, 1990; Buchanan and Oppenheim, 1968). The iep of kaolinite varies considerably depending on the source of the sample and the procedure used for cleaning the surface prior to study. Kitchener (1992) correctly points out that there is no one procedure for cleaning the surface of kaolinite and the surface properties depend critically on its prehistory.

Figure 4 shows the ζ and σ_0 of C18-kaolin as a function of pH and ionic strength with u-kaolin plotted for comparison. In contrast to u-kaolin, the ζ and σ_0 of

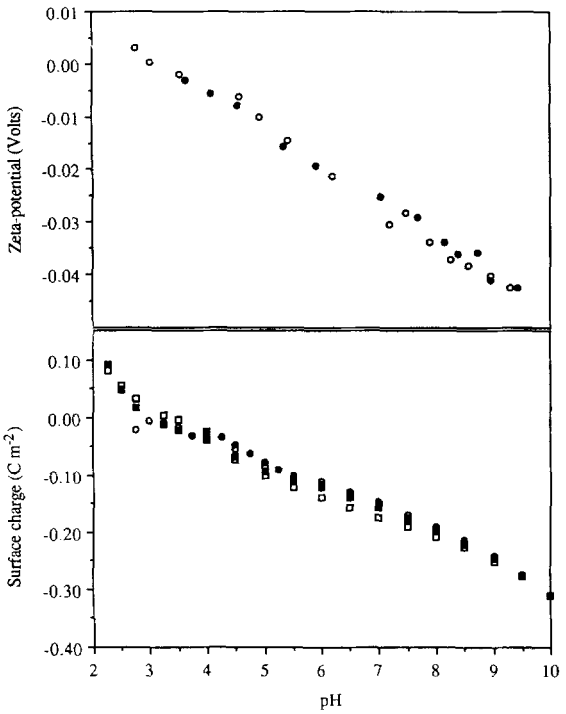

Figure 3. Zeta-potential (top) and surface charge (bottom) of u-kaolin as a function of pH and electrolyte concentration where (●) = 0.001 mol dm^{-3} KNO_3, (○) = 0.01 mol dm^{-3} KNO_3, (■) = 0.1 mol dm^{-3} KNO_3, and (□) = 1 mol dm^{-3} KNO_3.

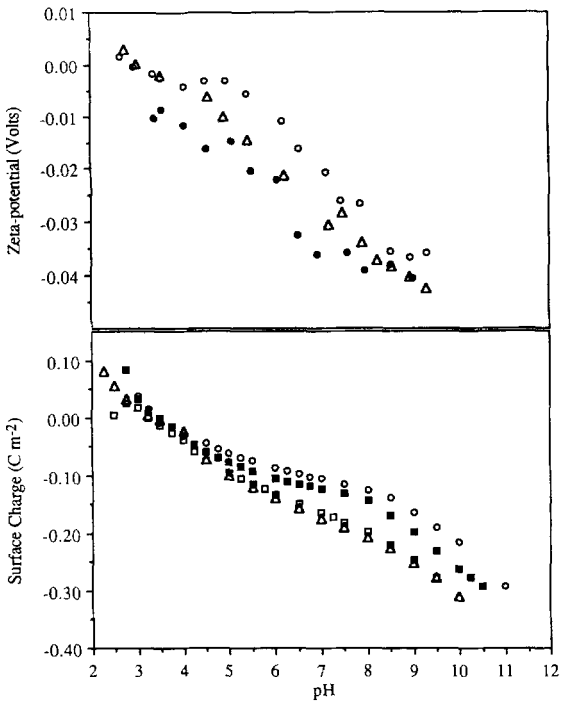

Figure 4. Zeta-potential (top) and surface charge (bottom) of C18-kaolin as a function of pH and electrolyte concentration compared with u-kaolin where (●) = C18-kaolin 0.001 mol dm^{-3} KNO_3, (○) = C18-kaolin 0.01 mol dm^{-3} KNO_3, (■) = C18-kaolin 0.1 mol dm^{-3} KNO_3, (□) = C18-kaolin 1 mol dm^{-3} KNO_3, (△) = u-kaolin 0.01 mol dm^{-3} KNO_3 for zeta-potential and 0.1 mol dm^{-3} KNO_3 for surface charge (u-kaolin plotted for comparison).

C18-kaolin samples exhibit a strong dependence on pH and electrolyte concentration. The σ_0 of the C18-kaolin progressively increases as the electrolyte concentration increases in general, is smaller in magnitude than for u-kaolin, but approaches more closely to the latter as the electrolyte concentration increases to 1 M and the pH falls below 4.5. The zeta potential of C18-kaolin is smaller in value at 0.01 mol dm^{-3} KNO_3 and larger at 0.001 mol dm^{-3} KNO_3 compared with the u-kaolin sample.

For the surface charge titration data of u-kaolin, the point of zero charge (pzc) was taken at pH 3 despite the absence of any defined common intersection point (cip) as there was no detectable change in σ_0 with electrolyte concentration. This choice was considered reasonable for both the isoelectric point (iep, zeta potential equals zero) and the pzc for the modified kaolinite, C18-kaolin, also occur at circa pH 3.

Rheology and sedimentation volumes

All of the kaolinite samples showed either Newtonian or pseudoplastic flow with no hysteresis. The extrapolated yield stress τ_β was obtained using the Bingham model (Tadros, 1989)

$$\tau = \tau_\beta + \eta_{pl}\dot{\gamma} \qquad (2)$$

where η_{pl}(N m^{-2} s) is the slope of the linear part of the line and the extrapolated yield stress τ_β is the shear rate extrapolated to $\dot{\gamma} = 0$.

Figure 5 shows the extrapolated yield stress τ_β as a function of pH and electrolyte concentration for u-kaolin and C18-kaolin. There are outstanding differences between the two samples. The u-kaolin samples show an increase in τ_β with a decrease in pH at all ionic strengths with a sharp rise in the τ_β for all curves at approximately pH = 5.25. There is also a common intersection point (cip) at this pH for all ionic strengths up to 0.1 mol dm^{-3} KNO_3, in which the τ_β increases with an increase in ionic strength above this pH and decreases with an increase in ionic strength below this pH. These results are similar to those obtained by Diz and Rand (1989).

The C18-kaolin samples show an increase in τ_β with a decrease in pH at all ionic strengths, as does the u-kaolin, but with the τ_β increasing more rapidly below a pH of approximately 7, as compared with 5.25 with the u-kaolin. In contrast to the u-kaolin, there is no common intersection point and the τ_β decreases with an increase in ionic strength at all pH values. Although the C18-kaolin does not exhibit a common intersection

https://doi.org/10.1346/CCMN.1994.0420203 Published online by Cambridge University Press

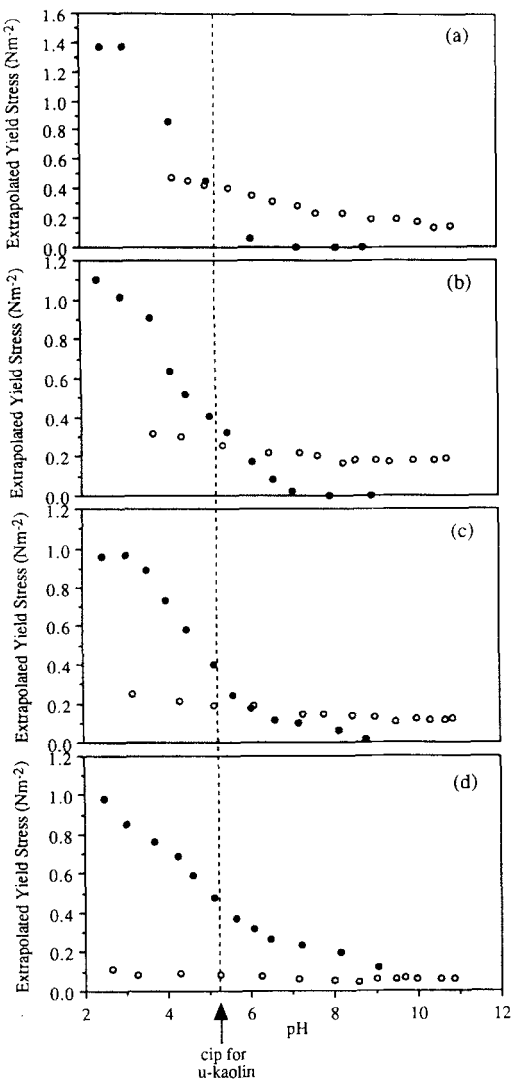

Figure 5. Extrapolated yield stress τ_β as a function of pH for C18-kaolin compared with u-kaolin, (●) = u-kaolin, (○) = C18-kaolin, where a) indicates no electrolyte, b) 0.001 mol dm^{-3} KNO_3, c) 0.01 mol dm^{-3} KNO_3, and d) 0.1 mol dm^{-3} KNO_3 u-kaolin and 0.05 mol dm^{-3} KNO_3 C18-kaolin. Note the common intersection point (cip) for u-kaolin at pH = 5.25.

point in the rheology data, there is an inflection point at pH = 6.75 in the surface charge–pH data (Figure 4).

The common intersection point in the u-kaolin rheology data and the inflection point in the C18-kaolin surface charge–pH data are assumed to be close to the isoelectric point of the edges (Diz and Rand, 1989). The edge isoelectric point is taken to occur at pH = 5.25 for u-kaolin and at pH = 6.75 for C18-kaolin in subsequent electrical double layer modeling. This value for the edge isoelectric point of kaolinite is similar to values cited by other workers (Williams and Williams, 1978; Diz and Rand, 1989).

The sedimentation volume results confirm the edge isoelectric point determined for u-kaolin from the extrapolated yield stress measurements. Figure 6 shows the sedimentation volumes as a function of pH and electrolyte concentration for u-kaolin. The curves show the same trends as those obtained for the extrapolated yield stress measurements also having a common intersection point between pH 5 and 5.5.

DISCUSSION

Electrical double layer site-binding model

The experimental data in this study are described assuming that the kaolinite surface behaves as an amphoteric oxide, where the electrical double layer (edl) properties are due to different surface sites on the basal planes and edges, represented here by SOH viz:

$$SOH_2^+ \overset{K_{a_1}^{int}}{\Leftrightarrow} SOH \overset{K_{a_2}^{int}}{\Leftrightarrow} SO^-$$

In this study we have assumed that there is a permanent negative charge on the basal planes of kaolinite, due to isomorphic substitutions rather than to gel coatings, as the particles used in this study have been cleaved to expose fresh surfaces and then water washed. Further, since kaolinite is a well-structured, non-porous oxide, a site-binding approach (Hunter, 1987) has been used to describe the experimental data. Two of the site-binding models, the Stern model and the triple layer model, have been employed to describe the electrical double layer of these kaolinite samples in order to determine if one model or the other better represents the data. The relevant equations describing these models are summarized below (Hunter, 1987; Westall and Hohl, 1980; Wood *et al.*, 1990).

$$SOH + H^+ \overset{1/K_{a_1}^{int}}{\Leftrightarrow} SOH_2^+$$

$$\frac{1}{K_{a_1}^{int}} = \frac{[SOH_2^+]}{[SOH][H^+]} \exp(e\Psi_0/kT) \qquad (3)$$

$$SOH \overset{K_{a_2}^{int}}{\Leftrightarrow} SO^- + H^+$$

$$K_{a_2}^{int} = \frac{[SO^-][H^+]}{[SOH]} \exp(-e\Psi_0/kT) \qquad (4)$$

Electrolyte counterions are attracted by an electrostatic potential, Ψ_β, and a chemical adsorption potential, Φ, to the inner Helmoltz plane, IHP, with the center of the ions at a distance β from the surface. They form complexes with the surface-charged groups resulting in a charge, σ_β, at the IHP. The ion complex equilibrium constants, $K_{NO_3^-}^{int}$ and $K_{K^+}^{int}$, representing the affinity of the electrolyte ions for the surface-charged groups are:

$$SOH_2^+ + NO_3^- \overset{K_{NO_3^-}^{int}}{\Leftrightarrow} SOH_2^+ - NO_3^-$$

https://doi.org/10.1346/CCMN.1994.0420203 Published online by Cambridge University Press

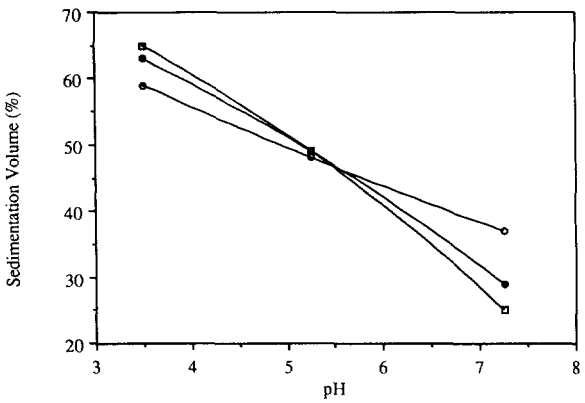

Figure 6. Sedimentation volumes (%) of u-kaolin as a function of pH. (□) = no electrolyte. (●) = 0.001 mol dm^{-3} KNO_3. (○) = 0.01 mol dm^{-3} KNO_3.

$$K^{int}_{NO_3^-} = \frac{[SOH_2^+ - NO_3^-]}{[SOH_2^+][NO_3^-]} \exp(-e\Psi_\beta/kT) \quad (5)$$

$$SO^- + K^+ \overset{K^{int}_{K^+}}{\Leftrightarrow} SO^- - K^+$$

$$K^{int}_{K^+} = \frac{[SO^- - K^+]}{[SO^-][K^+]} \exp(e\Psi_\beta/kT) \quad (6)$$

For the purposes of the numerical computation, these equilibria are written as exchange reactions:

$$SOH + H^+ + NO_3^- \overset{1/{}^*K^{int}_{NO_3^-}}{\Leftrightarrow} SOH_2^+ - NO_3^-$$

$$\frac{1}{{}^*K^{int}_{NO_3^-}} = \frac{[SOH_2^+ - NO_3^-]}{[SOH][H^+][NO_3^-]} \exp\frac{e(\Psi_0 - \Psi_\beta)}{kT} \quad (7)$$

$$SOH + K^+ \overset{{}^*K^{int}_{K^+}}{\Leftrightarrow} SO^- - K^+ + H^+$$

$${}^*K^{int}_{K^+} = \frac{[SO^- - K^+][H^+]}{[SOH][K^+]} \exp\frac{e(\Psi_\beta - \Psi_0)}{kT} \quad (8)$$

so that

$${}^*K^{int}_{K^+} = K^{int}_{a_2} K^{int}_{K^+} \quad (9)$$

and

$${}^*K^{int}_{NO_3^-} = K^{int}_{a_1}/K^{int}_{NO_3^-} \quad (10)$$

The chemical adsorption potential for the electrolyte counterions is given by:

$$\Phi_{ion} = -kT \ln(55.5\ K^{int}_{ion}) \quad (11)$$

The outer Helmoltz plane, OHP, is the innermost plane of the diffuse layer and is located at a distance d from the surface where the potential is Ψ_d. This is taken to be the measured zeta potential, ζ (Hunter, 1987).

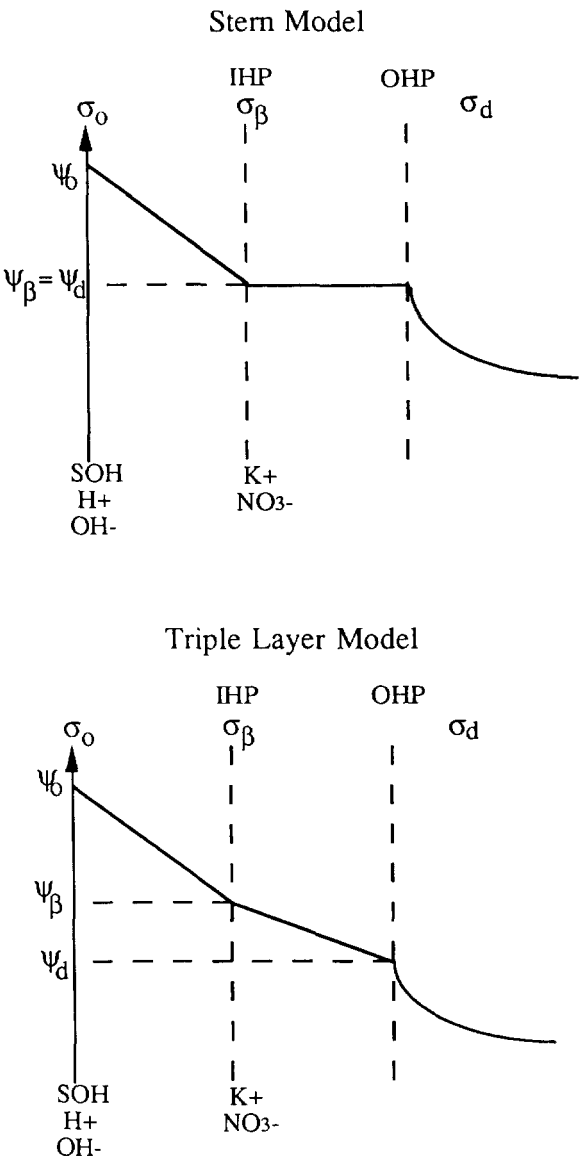

Figure 7. The electrical double layer around a particle for the Stern model and the triple-layer model.

The total number of sites on the kaolinite surface, N_s, is:

$$N_s = B([SOH] + [SOH_2^+] + [SOH_2^+ - NO_3^-] + [SO^-] + [SO^- - K^+]) \quad (12)$$

and the charges at the surface and the inner Helmoltz plane are:

$$\sigma_0 = B([SOH_2^+] + [SOH_2^+ - NO_3^-] - [SO^-] - [SO^- - K^+]) \quad (13)$$

$$\sigma_\beta = B([SO^- - K^+] - [SOH_2^+ - NO_3^-]) \quad (14)$$

https://doi.org/10.1346/CCMN.1994.0420203 Published online by Cambridge University Press

In order to satisfy electroneutrality constraints, these charges are compensated by the diffuse layer charge, σ_d:

$$\sigma_0 + \sigma_\beta + \sigma_d = 0 \quad (15)$$

where (Westhall and Hohl, 1980)

$$\sigma_0 = C_1(\Psi_0 - \Psi_\beta) \text{ and } \sigma_d = C_2(\Psi_d - \Psi_\beta) \quad (16)$$

and

$$\sigma_d = -\frac{2\epsilon\epsilon_0\kappa kT}{e}\sinh(Y_d/2)\left(1 + \frac{2}{\kappa a \cosh^2(Y_d/4)} + \frac{8\ln[\cosh(Y_d/4)]}{(\kappa a)^2\sinh^2(Y_d/2)}\right)^{1/2} \quad (17)$$

with the reciprocal double layer thickness $\kappa = ((2e^2N_A \cdot [KNO_3]10^3)/(\epsilon\epsilon_0 kT))^{1/2}$ and $Y_d = e\Psi_d/kT$ and where ϵ is the relative dielectric constant of the medium, ϵ_0 is the permittivity of vacuum, k is the Boltzmann's constant, T is the absolute temperature, e is the electrostatic charge of the counterions, N_A is the Avogadro number, and a is the radius of the kaolinite particle.

In Eq. 16, C_1 and C_2 are taken to be constant capacitances between the surface and the IHP and the IHP and OHP, respectively. In the basic Stern model, Ψ_β is set equal to Ψ_d and C_2 is ignored (Westall and Hohl, 1980). For the triple layer model, C_2 was chosen to be 0.2 F m^{-2}, a value often chosen for oxides (James and Parks, 1982).

A computer program was used to fit simultaneously the experimental data, with σ_0, ζ, pH, and $[KNO_3]$ as the variables. The adjustable parameters were chosen to be the pzc, $pK_{a_1}^{int}$, $p^*K_{NO_3^-}^{int}$, and C_1. The program uses a non-linear least squares subroutine to adjust simultaneously the value of the parameters until a minimum is found in the sums of the squares of the deviations between the experimental and calculated curves (Wood *et al.*, 1990).

$K_{a_1}^{int}$ and $K_{a_2}^{int}$ are linked to the pcz by:

$$pH_{pzc} = 1/2(pK_{a_1}^{int} + pK_{a_2}^{int}) \quad (18)$$

$\Delta pKa = pK_{a_2}^{int} - pK_{a_1}^{int}$ is an indication of the amount of charge present at the interface at the pzc, and the fraction of positive sites or negative sites (which are equal), ϕ_0, that are present at the pzc can be calculated according to Hunter (1987):

$$\Delta pKa = 2\,\text{Log}\frac{1 - 2\phi_0}{\phi_0} \quad (19)$$

As the iep and pzc were found to be the same experimentally, $pK_{NO_3^-}^{int}$ is set equal to $pK_{K^+}^{int}$ (i.e., symmetrically adsorbing electrolyte). The modeling was performed using both the surface charge and zeta potential results on two separate sets of data.

Firstly, the experimental data were used without modification; and the surface sites, SOH, were taken to be an average of the different surface sites at the edges, which are amphoteric and, thus, pH- and electrolyte-dependent, and the basal planes, which carry a permanent negative charge and are, therefore, pH-independent but electrolyte-dependent. N_s was estimated using the CEC of 3.1 meq 100 g^{-1} and the measured surface area of 15.3 $m^2\,g^{-1}$. It was found that the choice of N_s was insensitive in the fitting process; the value used for the calculations was 1.2×10^{18} sites m^{-2}.

Secondly, the surface charge and zeta potential contribution due to the basal planes' constant negative charge were subtracted out of all of the data, effectively removing the SO^- basal planes' sites contribution and the surface sites, SOH, were taken to be the edge sites only (Figure 1a). This effectively makes $K_{a_1}^{int}$ the equilibrium constant for the dissociation of the alumina surface hydroxyl group, $Al(OH)(OH_2)^+$, and $K_{a_2}^{int}$ the equilibrium constant for the dissociation of the silica surface hydroxyl site, SiOH. The contribution subtracted due to the constant charge of the basal planes was determined for each ionic strength by making the surface charge and the zeta potential zero at the pH of the edge isoelectric points determined from the rheological measurements for u-kaolin and the inflection point of the surface charge–pH curve for C18-kaolin, (i.e., at pH = 5.25 for u-kaolin and pH = 6.75 for C18-kaolin). The N_s value used for these data, 4.7×10^{18} sites m^{-2}, was calculated by taking the average of the SiOH sites for silica, 4.6×10^{18} sites m^{-2}, and the AlOH edge sites of alumina, 4.7×10^{18} sites m^{-2} (Hiemstra *et al.*, 1989). The surface area was taken as 10% of the whole surface area, 1.53 $m^2\,g^{-1}$, as the edges only occupy approximately 10% of the kaolinite surface (Wierer and Dobias, 1988). The N_s value was kept constant between u-kaolin and C18-kaolin as this was again found to be an insensitive parameter in the fitting process.

The best fit between experimental data and theory was obtained using the basic Stern model. The use of more complicated models such as the triple layer case, or invoking two types of amphoteric surface groups at the edges, did not improve the "goodness of fit"; thus, the simplest model was chosen. The calculated and experimental curves for the basic Stern model before and after subtraction of the contribution due to the basal planes are compared in Figures 8 and 9 for u-kaolin and Figures 10 and 11 for C18-kaolin. In all samples, the calculated σ_0 values as a function of pH and electrolyte concentration show better agreement with the experimental data than the calculated Ψ_d values do with ζ measurements, particularly at the higher ionic strength of 0.01 mol dm^{-3}. Koopal *et al.* (1987) found similar results. This could have two causes. Firstly, by taking $\Psi_d = \zeta$, we are assuming that the position of the plane of shear at which ζ is measured is at d. Secondly, both the measurement of electrophoretic mobility and the calculation of ζ from electrophoretic mobility as-

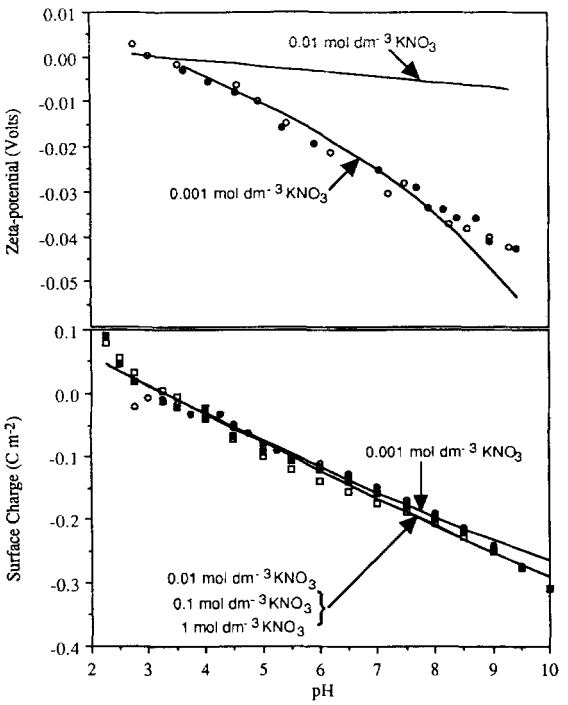

Figure 8. The calculated and experimental curves of zeta potential (top) and surface charge (bottom) as a function of pH and electrolyte concentration using the basic Stern model before subtraction of the contribution due to the basal planes for u-kaolin. The calculated curves are solid lines (——) labeled with the electrolyte concentration. The experimental curves are plotted as (●) = 0.001 mol dm^{-3} KNO_3, (○) = 0.01 mol dm^{-3} KNO_3, (■) = 0.1 mol dm^{-3} KNO_3, and (□) = 1 mol dm^{-3} KNO_3.

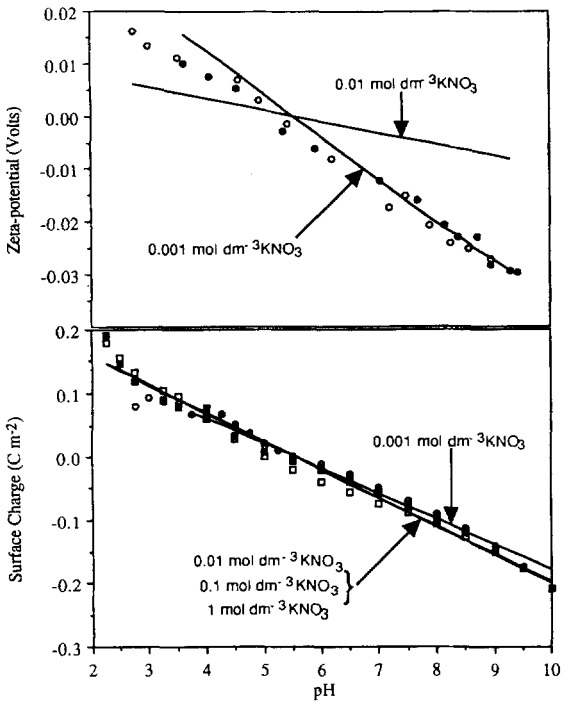

Figure 9. The calculated and experimental curves of zeta potential (top) and surface charge (bottom) as a function of pH and electrolyte concentration using the basic Stern model after subtraction of the contribution due to the basal planes for u-kaolin. The calculated curves are solid lines (——) labeled with the electrolyte concentration. The experimental curves are plotted as (●) = 0.001 mol dm^{-3} KNO_3, (○) = 0.01 mol dm^{-3} KNO_3, (■) = 0.1 mol dm^{-3} KNO_3, and (□) = 1 mol dm^{-3} KNO_3.

sume a spherical particle with a uniform homogeneous surface. Kaolinite consists of flat plate-like particles with different atomic environments on each of the basal planes and the edges, hence the electrical double layer will vary around the particle. This means that the measurement of electrophoretic mobilities produces an "average" and the subsequent calculation of ζ is very complex. Despite these problems, the model shows no significant change in surface charge with ionic strength for the u-kaolin, but indicates a change in surface charge with ionic strength for the C18-kaolin. The model has not been able to show that ζ is invariant with ionic strength for the u-kaolin.

Table 1 lists the best-fit parameters calculated for the surface-charge and zeta-potential data for both the u-kaolin and C18-kaolin before and after the subtraction of the contribution due to the basal planes. The calculated parameters, after the subtraction of the contribution due to the basal planes, permit two quantitative comparisons to be made. Firstly, a comparison of the electrical double layer parameters calculated for the u-kaolin in this study to other studies on oxides and clay minerals enables assignments of Ka_1 and Ka_2 to be made to specific chemical groups on the surface of kaolinite. Secondly, a comparison is made between the charging behavior and the electrical double layer properties of the u-kaolin and the silane modified C18-kaolin in aqueous solutions.

The acidity constants obtained for the u-kaolin sample after the basal plane contribution has been subtracted correlate very closely with values determined for the most acidic sites from studies of silica and alumina. As already mentioned, once the contribution due to the basal planes has been subtracted, the acidity constants can be assigned to specific chemical groups on the edges of the surface as shown in Figure 1a and can be represented as follows:

$$Al(OH)(OH_2)^+ \overset{K_{a_1}^{int}}{\Leftrightarrow} Al(OH)(OH) + H^+ \text{ and}$$

$$SiOH \overset{K_{a_2}^{int}}{\Leftrightarrow} SiO^- + H^+ \qquad (20)$$

Table 2 summarizes the correlation between the acidity constants and ion complex constants obtained from other studies to the values calculated in this study. There is an excellent correlation between the $pK_{a_1}^{int}$ value of 5.0 calculated for kaolinite here and the most

https://doi.org/10.1346/CCMN.1994.0420203 Published online by Cambridge University Press

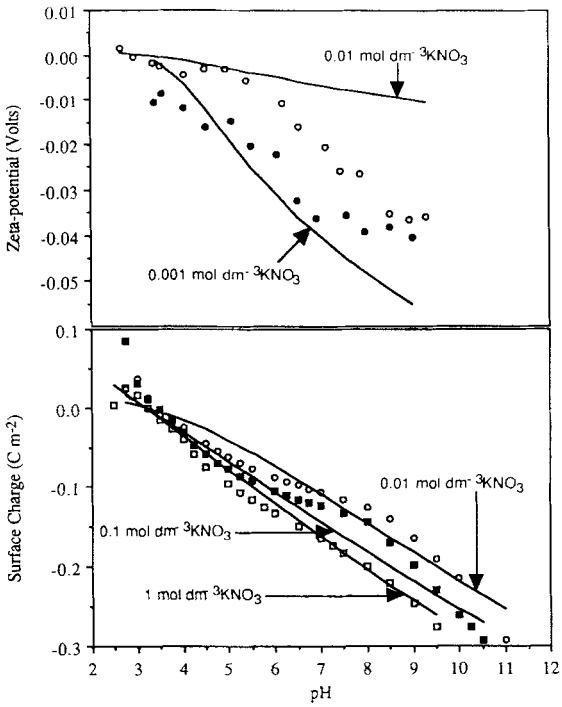

Figure 10. The calculated and experimental curves of zeta potential (top) and surface charge (bottom) as a function of pH and electrolyte concentration using the basic Stern model before subtraction of the contribution due to the basal planes for C18-kaolin. The calculated curves are solid lines (——) labeled with the electrolyte concentration. The experimental curves are plotted as (●) = 0.001 mol dm^{-3} KNO_3, (○) = 0.01 mol dm^{-3} KNO_3, (■) = 0.1 mol dm^{-3} KNO_3, (□) = 1 mol dm^{-3} KNO_3.

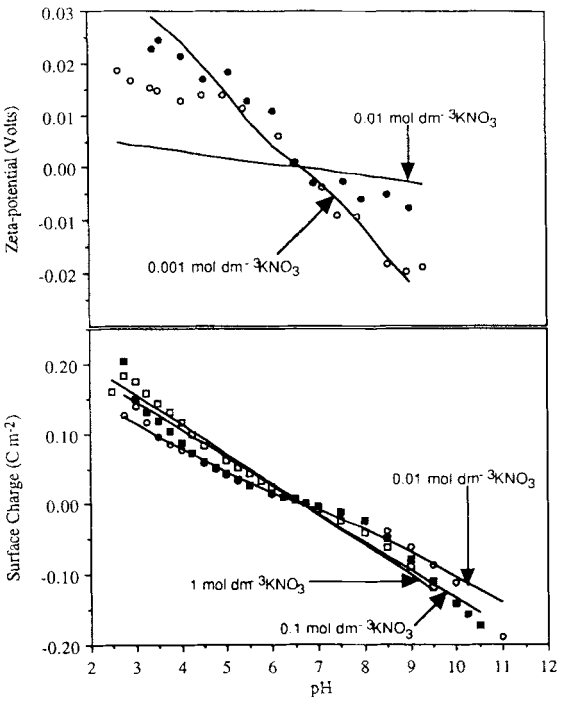

Figure 11. The calculated and experimental curves of zeta potential (top) and surface charge (bottom) as a function of pH and electrolyte concentration using the basic Stern model after subtraction of the contribution due to the basal planes for C18-kaolin. The calculated curves are solid lines (——) labeled with the electrolyte concentration. The experimental curves are plotted as (●) = 0.001 mol dm^{-3} KNO_3, (○) = 0.01 mol dm^{-3} KNO_3, (■) = 0.1 mol dm^{-3} KNO_3, and (□) = 1 mol dm^{-3} KNO_3.

acidic pKa value of 5.24 and 5.2 published for the alumina studies (James and Parks, 1982; Pulfer *et al.*, 1984) as well as the $pK_{a_2}^{int}$ value of 6.0 calculated for kaolinite here and the most acidic pKa value of 6.53 published for the silica SiOH studies (Schindler and Stumm, 1987). The ion complex constant of 7.7 for the anion for kaolinite correlates well with that obtained for the alumina studies value of 7.9 even though the anion in each study was different. The capacity values calculated in this study, of 0.78 C F m^{-2}, are of the same high magnitude as the alumina studies (0.90 C F m^{-2}).

James and Parks (1982) have modeled clay minerals assuming the existence of two types of acidic surface sites: a strongly acidic site, SOH, and a weaker acidic site, TOH. One weakness of this approach is that no chemical assignment is made to these groups and the total concentrations of each site, [SOH] and [TOH], varied with electrolyte cation. This model assumes that the clay surfaces do not develop a positive charge, nor a point of zero charge, in the pH range of 3.5 to 11 considered. This correlates with the data in this study. The calculated acidity and ion binding constants for the more acidic site, as determined by this model for a Putnam clay, are shown in Table 2. There is a strong correlation between the pKa values of 6.8 and 6.0 calculated for the Putnam clay and the $pK_{a_2}^{int}$ value of 6.0 calculated for the SiOH site here as well as between the $p^*K_{cation}^{int}$ values of 3.2 and 3.0 calculated for the Putnam clay and the $p^*K_{K^+}^{int}$ of 3.4 calculated for kaolinite in this study.

Studies on mica by Scales *et al.* (1990), using a single site dissociation model to model zeta potential data at various ionic strengths and a pH = 5.8, produced a pKa value of 5.6, which is the average of the $pK_{a_1}^{int}$ and $pK_{a_2}^{int}$ values in this study for kaolinite, and a $p^*K_{K^+}^{int}$ of 3.2, which is almost identical to the value calculated for kaolinite (Table 2). Mica is also an aluminosilicate clay mineral (both basal planes have the siloxane inert structure) which carries a permanent negative charge due to isomorphic substitution of one in four Si for Al. Scales *et al.* (1990) used extremely high values for capacities C_1 and C_2 of 10 F m^{-2} and 2 F m^{-2}, respectively. They also found similar limitations with the model, particularly with the high chemical adsorptions of the counterions, (ϕ), which they found to be of the

https://doi.org/10.1346/CCMN.1994.0420203 Published online by Cambridge University Press

Table 1. Parameter calculated using the basic Stern model for u-kaolin and C18-kaolin.

	u-kaolin[1] Stern model	C18-kaolin[1] Stern model	u-kaolin[2] Stern model (basal plane contribution subtracted)	C18-kaolin[2] Stern model (basal plane contribution subtracted)
$pK_{a_1}^{int}$	2.5	−0.32	5.0	2.9
$pK_{a_2}^{int}$	4.1	6.7	6.0	10.4
$p^*K_{NO_3}^{int}$	6.6	3.4	7.7	6.8
$p^*K_{K^+}^{int}$	0	2.9	3.4	6.5
$pK_{ion}^{int} = pK_{NO_3^-}^{int} = pK_{K^+}^{int}$	−4.1	−3.8	−2.7	−4.0
ΔpKa	1.6	7.0	1.0	7.5
$\Delta p^*K_{complex}^{int}$	−6.6	−0.5	−4.3	−0.3
C_1 (F m^{-2})	0.81	0.78	0.78	0.75
pzc	3.3	3.2	5.5	6.7
Φ_{ion}	−13kT	−13kT	−10kT	−13kT
ϕ_0	0.11	3.2×10^{-4}	0.19	1.6×10^{-4}

[1] Before subtracting the zeta-potential and surface charge contribution due to the basal planes.
[2] After subtraction of the zeta-potential and surface charge contribution due to the basal planes.

same order of −10kT as has been found here. Hunter (1987, 1981) points out that high chemical adsorptions of the counterions are expected as the surface charge on the mineral is high, but the measured zeta potentials are very low for this high surface charge. Nevertheless, these values are still unreasonably high for ions that are meant to be nonspecifically adsorbing, which could be due to the fact that the model does not consider the charge in the IHP to be discrete, but rather assumes that there is a uniform charge density.

Other studies of kaolinite in which acidity constants have been calculated include works in which acid-base titrations at various ionic strengths are used to determine multiple proton functional groups on the kaolinite surface. Kramer *et al.* (1991) have determined a series of acidity constants for a sample of unpurified Macon, Georgia, kaolinite using a multiple discrete functional site analysis in which it is assumed that there is one metal ion in the kaolinite lattice and there are discrete equal pK interval sites. They determined four pK values of about 4.6, 6.7–7.3, 8.7–10, and 2.8–3.4 from acid-base and base-acid titrations in the pH range 3–11 and ionic strengths of 0.005, 0.05, 0.5 mol dm^{-3} KCl. The first three pK values are assigned to various alumina sites on the edges and basal planes, and the fourth value is assigned to an ion exchange reaction for a silanol layer. Although the assignment of the pK values is somewhat different from this study, the values correlate reasonably well with the four binding constants, $pK_{a_1}^{int}$, $pK_{a_2}^{int}$, $p^*K_{K^+}^{int}$ and $p^*K_{Na^+}^{int}$, calculated in this study.

On comparing the values calculated before and after subtraction of the contribution due to the basal planes (Table 1), the values of pKa and $p^*K_{ion}^{int}$ before the subtraction reflect the inclusion of a permanent negative site which can be considered to be a very acidic site, thereby making the pKa values more acidic as these values are taken as an average of these sites. It is important to note that ΔpKa, $\Delta p^*K_{complex}^{int}$, C_1, Φ, and ϕ_0 are of the same magnitude. The advantage of subtracting the contribution due to the basal planes is that acidity constants can be assigned more accurately to specific chemical groups on the surface. This applies not only to the u-kaolin, but also to the silane modified sample, C18-kaolin.

The silane molecules have clearly interacted in some way with the pH-dependent sites on the edges as the charge and electrophoretic mobility as a function of pH and electrolyte concentration are affected by the modification. This is reflected in the values of the acidity constants calculated. In both sets of data, the $pK_{a_1}^{int}$ has decreased while $K_{a_1}^{int}$ increased and $pK_{a_2}^{int}$ has increased while $K_{a_2}^{int}$ decreased. If these values are assigned to the same chemical groups as the u-kaolin, then this indicates that the acidity of the edge groups has been affected by the presence of the silane molecules, causing a decrease in the ionization of the edge groups. This is shown quantitatively by a large increase in the ΔpKa value from approximately 1 for the u-kaolin to 7 for the C18-kaolin and a decrease in the fraction of positive sites or negative sites, ϕ_0, that are present at the pzc from approximately 10^{-1} to 10^{-4}. As mentioned earlier, it is the hydroxyl groups at the edges that are considered to be the major sites of kaolinite's reactivity and this can be depicted as one or more of the products shown in Figure 1b.

Stumm *et al.* (1970) point out that the acidity of surface OH groups of hydrous oxides depends on three factors: the acidity of the metal ion; the influence of the electrostatic field and induction effects of the solid; and the structural ordering of the water layer immediately adjacent to the solid surface. The attachment of a hydrophobic organic alkyl silane is expected to perturb both the electrostatic field of the solid at the surface as well as the structural ordering of the water layer immediately adjacent to the solid surface in such

Table 2. A comparison of the acidity and complex ion equilibrium constants from different studies of alumina, silica, and mixed oxide minerals.

Comments	Solid	Ionic medium	$pK_{a_1}^{int}$	$pK_{a_2}^{int}$	$p^*K_{cation}^{int}$	$p^*K_{anion}^{int}$	C F m $^{-2}$	Reference
Values calculated from electrophoresis and surface charge titrations in this study for edge sites, as basal plane contribution subtracted, using Stern model.	kaolinite	KNO_3	5.0	6.0	3.4	7.7	0.78	This study
For Group Al(OH)(OH_2)	γ-Al(OH)$_3$	1M KNO_3	5.24					Pulfer *et al.* (33)
For Group Si-OH	SiO_2(am)	0.2M KNO_3		6.53				Schindler & Stumm (34)
Calculated from electrophoresis and surface charge measurements using a surface complexation model.	γ-Al_2O_3	0.001, 0.01, 0.1M NaCl	5.2		9.2 (Na^+)	7.9 (Cl^-)	0.90 C_2 = 0.2	James & Parks (3)
The stronger acidic site of the two types of acidic surface sites modeled for a Putnam clay surface.	Putnam Clay (Electrodialysed in H form)							
These ionization and complexation constants were used to model experimental NaOH titration curves using a simple ion-exchange model in which the electrical double layer was not considered.				6.8	3.2 (Na^+)			James & Parks (3)
These ionization and complexation constants were used to model experimental NaOH titration curves and to calculate zeta potential curves using an electrical double layer model.				6.0	3.0		2.50	James & Parks (3)
Fit zeta potential data at pH = 5.8 using a single site dissociation model.	Mica	KCl		5.6 (average of pKa_1 & pKa_2 of kaolinite)	3.2		10 C_2 = 2	Scales *et al.* (35)

a way as to cause a decrease in the capacity for ionization of the adjacent surface hydroxyl groups (Israelachvili, 1992). The values calculated for the various parameters (Table 1) support this explanation and the idea that the organosilane reacts with the pH-dependent hydroxyl surface groups on the edges of the kaolinite surface. Furthermore, the C18-kaolin particles are easily dispersed, and electrophoretic mobility and surface charge measurements were readily performed. This indicates that the silane has not attached over the entire kaolinite surface, suggesting that the silane has reacted only with a fraction of the surface, i.e., the edges.

SUMMARY

Electrochemical and rheological data have provided detailed information of the charging behavior of both an unmodified and long chain silane-modified kaolinite in aqueous dispersions, providing evidence for the acidity and location of the reactive hydroxyl groups on the surface and the interaction of these groups with water and the organosilane.

The Stern model of the electrical double layer has been successfully applied to assign Ka_1 and Ka_2 values to specific chemical groups on the surface of kaolinite and to examine quantitatively the influence of the modification of the surface of kaolinite with an organosilane on the charging of the surface in aqueous solutions. With the removal of the constant negative charge contribution on the basal planes, the calculated acidity and ion complex constants indicate that the acidity constants Ka_1 and Ka_2 refer to the pH-dependent alumina edge and silica edge sites, respectively, and that the silane has reacted with the surface in such a way as to decrease the extent of ionization of these groups with the consequence that the overall surface charge has decreased at ionic strengths less than 1 M. The infrared data provide evidence that the silane molecules are bound tightly to the surface as they are not removed by washing with cyclohexane, heating at 110°C, or dispersion in aqueous solutions. It has been shown that organosilanes react with surface ionizable hydroxyl groups at the edges and are held by strong bonding.

At high ionic strengths, the C18-kaolin has low extrapolated yield stress values over all pH values that do not change significantly with pH. This may have industrial importance as it means that there is an insignificant change in the flocculation behavior with pH and suggests that there is very little buildup of the structure that is predominant in unmodified kaolinite dispersions at high ionic strengths and low pH.

ACKNOWLEDGMENTS

Discussions with Dr. Clive Prestidge are warmly acknowledged. Financial support from the Australian Research Council and Westralian Sands Ltd. is gratefully acknowledged.

REFERENCES

Bolland, M. D. A., Posner, A. M., and Quirk, J. P. (1980) pH-Independent and pH-dependent surface charges on kaolinite: *Clays & Clay Minerals* **28,** 412–418.

Buchanan, A. S. and Oppenheim, R. C. (1968) The surface chemistry of kaolinite: *Aust. J Chem.* **21,** 2367–2371.

de Bruyn, P. L. and Agar, G. E. (1962) Surface chemistry of flotation: in *Froth Flotation,* D. W. Fuerstenau, ed., 50th Anniversary Volume, AIME, New York, 91–134.

de Keizer, A. (1990) Adsorption of paraquat ions on clay minerals. Electrophoresis of clay particles. *Progr. Colloid Polym. Sci.* **83,** 118–126.

Diz, H. M. M. and Rand, B. (1989) The variable nature of the isoelectric point of the edge surface of kaolinite: *Br. Ceram. Trans. J.* **88,** 162–166.

Greenland, D. J. and Mott, C. J. B. (1978) Surfaces of soil particles: in *The Chemistry of Soil Constituents,* D. J. Greenland and M. B. H. Hayes, eds., John Wiley & Sons, New York, 330–333.

Hair, M. L. (1986) Silica surfaces: in *Silanes, Surfaces and Interfaces,* D. E. Leyden, ed., Gordon and Breach Science Publishers, New York, 25–41.

Hiemstra, T., de Witt, J. C. M., and van Riemsdijk, W. H. (1989) Multisite proton adsorption modeling at the solid/solution interface of (hydr)oxides: A new approach: *J. Colloid Interface Sci.* **133,** 105–117.

Hunter, R. J. (1981) *Zeta Potential in Colloid Science:* Academic Press, London, 298 pp.

Hunter, R. J. (1987) *Foundations of Colloid Science, Vol. I:* Oxford University Press, New York, 316–394, p. 557.

Hurlbut, C. S. Jr. (1971) *Dana's Manual of Mineralogy,* 18th ed.: John Wiley & Sons, New York, 426 pp.

Israelachvili, J. (1992) *Intermolecular and Surface Forces,* 2nd ed.: Academic Press, London, 128–133.

James, R. O. and Parks, G. A. (1982) Characterization of aqueous colloids by their electrical double-layer and intrinsic surface chemical properties: in *Surface and Colloid Science, Vol. 12,* E. Matijević, ed., Plenum, New York, 119–216.

Jepson, W. B. (1984) Kaolins: Their properties and uses: *Phil. Trans. R. Soc. Lond.* **A 311,** 411–432.

Kitchener, J. A. (1992) Minerals and surfaces: in *Developments in Mineral Processing, Vol. 12: Colloid Chemistry in Mineral Processing,* J. S. Laskowski and J. Ralston, eds., Elsevier Science Publishers B.V., Amsterdam, p. 30.

Koopal, L. K., van Riemsdijk, W. H. and Roffey, M. G. (1987) Surface ionization and complexation models: A comparison of methods for determining model parameters: *J. Colloid Interface Sci.* **118,** 117–136.

Kramer, J. R., Collins, P., and Brassard, P. (1991) Characterization of multiple functional groups on kaolinite: *Mar. chem.* **36,** 1–8.

Messerschmidt, R. G. (1985) Complete elimination of specular reflectance in infrared diffuse reflectance measurements: *Appl. Spectr.* **39,** 737–794.

Morris, H. D., Shelton, B., and Ellis, P. D. (1990) ^{27}Al NMR spectroscopy of iron-bearing montmorillonite clays: *J. Phys. Chem.* **94,** 3121–3129.

Nguyen, T. T., Janik, L. J., and Raupach, M. (1991) Diffuse reflectance infrared fourier transform (DRIFT) spectroscopy in soil studies: *Aust. J. Soil Res.* **29,** 49–67.

Ohshima, H., Healy, T. W., and White, L. R. (1983) Approximate analytic expressions for the electrophoretic mobility of spherical colloidal particles and the conductivity

of their dilute suspensions: *J. Chem. Soc., Faraday Trans. 2* **79,** 1613–1628.

Pleuddemann, E. P. (1982) *Silane Coupling Agents:* Plenum Press, New York, p. 20.

Pulfer, K., Schindler, P. W., Westall, J. C., and Grauer, R. (1984) Kinetics and mechanism of dissolution of bayerite (γ-$Al(OH)_3$) in HNO_3-HF solutions at 298.2 °K: *J. Colloid Interface Sci.* **101,** 554–564.

Rand, B. and Melton, I. E. (1977) Particle interactions in kaolinite: *J. Colloid Interface Sci.* **60,** 308–329.

Scales, P. J., Grieser, F., and Healy, T. W. (1990) Electrokinetics of the muscovite mica-aqueous solution interface: *Langmuir* **6,** 582–589.

Schindler, P. W. and Stumm, W. (1987) The surface chemistry of oxides, hydroxides, and oxide minerals: in *Aquatic Surface Chemistry,* W. Stumm, ed., John Wiley & Sons, New York, p. 97.

Schofield, R. K. and Samson, H. R. (1954) Flocculation of kaolinite due to the attraction of oppositely charged crystal faces: *Discuss. Faraday Soc.* **18,** 135–144.

Socrates, G. (1980) *Infrared Characteristic Group Frequencies:* John Wiley & Sons, New York, p. 27.

Stumm, W., Huang, C. P., and Jenkins, S. R. (1970) Specific chemical interaction affecting the stability of dispersed systems: *Croat. Chem. Acta* **42,** 223–245.

Tadros, Th. F. (1989) Rheology of concentrated stable and flocculated suspensions: in *Flocculation and Dewatering Proc. of the Engineering Foundation Conf., Palm Coast, Florida,* B. M. Moudgil and B. J. Scheiner, eds., Engineering Foundation, New York, 43–87.

van Olphen, H. (1977) *An Introduction to Clay Colloid Chemistry,* 2nd ed.: John Wiley & Sons, New York, 92–110.

Westall, J. and Hohl, H. (1980) A comparison of electrostatic models of the oxide/solution interface: *Adv. Colloid Interface Sci.* **12,** 265–294.

Wierer, K. A. and Dobias, B. (1988) Exchange enthalpies of H^+ and OH^- adsorption on minerals with different characters of potential-determining ions: *J. Colloid Interface Sci.* **122,** 171–177.

Williams, D. J. A. and Williams, K. P. (1978) Electrophoresis and zeta potential of kaolinite: *J. Colloid Interface Sci.* **65,** 79–87.

Wood, R. (1990) The electrical double layer properties of oxides: Masters thesis, The South Australian Institute of Technology, 40–50.

Wood, R., Fornasiero, D., and Ralston, J. (1990) Electrochemistry of the boehmite-water interface: *Colloids Surf.* **51,** 389–403.

(Received 25 February 1993; accepted 13 October 1993; Ms. 2337)